

Dalton Transactions

Accepted Manuscript



This is an *Accepted Manuscript*, which has been through the Royal Society of Chemistry peer review process and has been accepted for publication.

Accepted Manuscripts are published online shortly after acceptance, before technical editing, formatting and proof reading. Using this free service, authors can make their results available to the community, in citable form, before we publish the edited article. We will replace this *Accepted Manuscript* with the edited and formatted *Advance Article* as soon as it is available.

You can find more information about *Accepted Manuscripts* in the [Information for Authors](#).

Please note that technical editing may introduce minor changes to the text and/or graphics, which may alter content. The journal's standard [Terms & Conditions](#) and the [Ethical guidelines](#) still apply. In no event shall the Royal Society of Chemistry be held responsible for any errors or omissions in this *Accepted Manuscript* or any consequences arising from the use of any information it contains.

Cite this: DOI: 10.1039/c0xx00000x

www.rsc.org/xxxxxx

ARTICLE TYPE

Novel iminopyridine derivatives: ligands for preparation of Fe(II) and Cu(II) dinuclear complexes

Oriol Martínez-Ferraté,^{a,b} Josep M. López-Valbuena,^a Marta Martínez Belmonte,^a Andrew J. P. White,^c Jordi Benet-Buchholz,^a George J. P. Britovsek,^c Carmen Claver^{*b,d} and Piet W. N. M. van Leeuwen^{*a}

Received (in XXX, XXX) Xth XXXXXXXXX 20XX, Accepted Xth XXXXXXXXX 20XX

DOI: 10.1039/b000000x

A series of imino- and amino-pyridine ligands based on dihydrobenzofurobenzofuran (BFBF) and methanodibenzodioxocine (DBDOC) backbones have been synthesized. These ligands form exclusively dinuclear complexes with metals such as iron(II) and copper(II). The structures for complexes **15**, **16**, **18**, **19**, **20**, **21**, **23**, and **24** were determined by X-ray crystallography. The complexes show large distances for the metal nuclei and different geometries depending on the nature of the metal. An octahedral geometry was observed for the iron(II) complexes, while copper (II) complex **24** showed a distorted trigonal bipyramidal geometry. The iron (II) complexes showed activity as catalysts in the cycloaddition of CO₂ to epoxides, obtaining moderate yields of cyclic carbonates.

15 Introduction

Dinuclear and multinuclear metallic centres play an important role in biochemical processes such as oxygen transport and photosynthesis.¹⁻⁷ For several metalloproteins the active sites are composed of metal clusters.¹⁻⁷ The reactivity of the bimetallic proteins differs considerably from known coordination compounds. An example is methane monooxygenase (diiron active centre) which is able to activate methane to undergo oxidation to methanol without further oxidation.^{5,6,8}

Bimetallic compounds are also known in organometallic chemistry, for instance halide- or methoxide-bridged compounds are common starting materials in the synthesis of organometallic compounds.⁹⁻¹² Unfortunately, donor ligands may cause cleavage of the bridging species and we may lose the bimetallic nature.^{10,13-16} Likewise in metalloproteins, bimetallic species often show properties different from those of homologous single metal compounds. As for homogeneous catalysts, bimetallic compounds can be more effective catalyst than monometallic complexes in some reactions.¹⁶⁻²² Examples are catalysts for methanol carbonylation, copolymerization of epoxides and carbon dioxide, and olefin metathesis. The change in activity is attributed to a cooperative effect between the two metal centres which is possible when they are in close proximity (often less than 5 Å apart).²³⁻³³

Several of these active species are formed *in situ* when the components are brought together in solution. In order to enforce the formation of bimetallic compounds rather than being dependent on their accidental formation, we can use ligand design to achieve this goal. This means that in the designed framework the metals should be close enough to show a cooperative effect. Several strategies have been used in the design of ligands that promote the formation of bimetallic compounds and a few of

these are presented in Fig. 1.^{20,25,34-40}

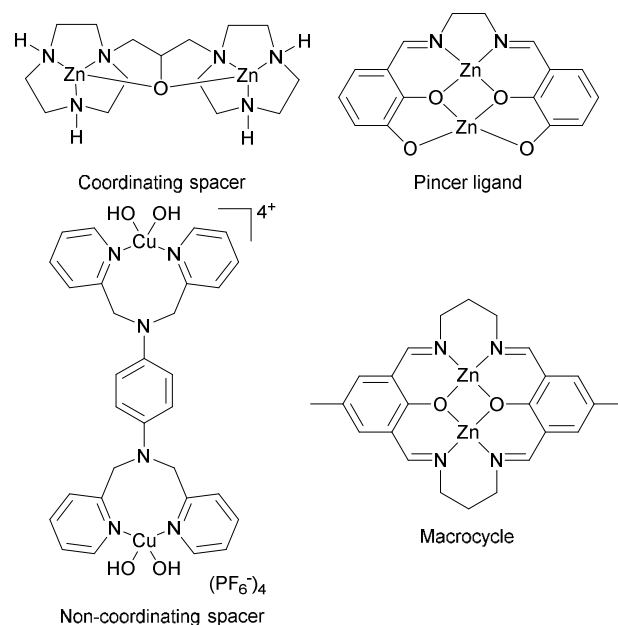


Fig. 1 Examples of designed bimetallic complexes

Numerous cooperative effects have been observed for designed dinuclear complexes applied in homogeneous catalytic reactions.⁴¹ For instance, copper dinuclear systems were applied in oxidative phenol coupling or azide-alkyne cycloadditions with high activities and selectivities for both reactions.⁴²⁻⁴⁴ Zinc dinuclear complexes were applied in various reactions with excellent results, for example desymmetrization of *meso*-diols or asymmetric aldol reaction.^{45,46} The catalytic synthesis of cyclic carbonates was shown to involve

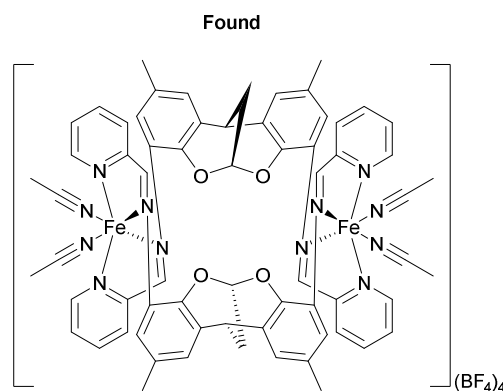
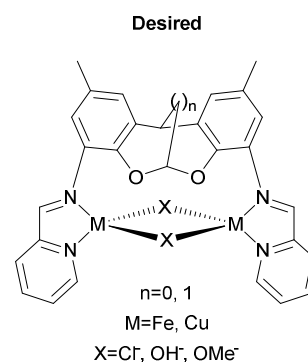
multinuclear systems of zinc or aluminum which show enhanced rates due to cooperative effects.^{36,47,48} This reaction has been less well-studied with the use of iron complexes and only a few examples have been reported.^{49–56} There is no example of
 5 dinuclear iron (II) complexes applied in this reaction.

Results and discussion

Our group previously reported the capability of benzofurobenzofuran (BFBF) and methanodibenzodioxocine (DBDOC) bisphosphine derivatives to form dinuclear complexes with rhodium. It was demonstrated that these dinuclear complexes gave higher rates in methanol carbonylation than their monometallic analogues.²⁰ Here we report on the tetranitrogen derivatives based on these two backbones with the intention to
 10 prepare dinuclear complexes as shown in Fig. 2. Despite our efforts to synthesized bimetallic bridged compounds, the final complexes presented a total different geometry.

Ligand syntheses

Scheme 1 summarizes the synthetic pathways to ligands **6–14**. Ligands **6–12** and **14** present a C_s -symmetry and they were designed to form dinuclear complexes with various metals. In contrast, ligand **13** has C_1 -symmetry and is used as monometallic reference to check for cooperative effects.
 20



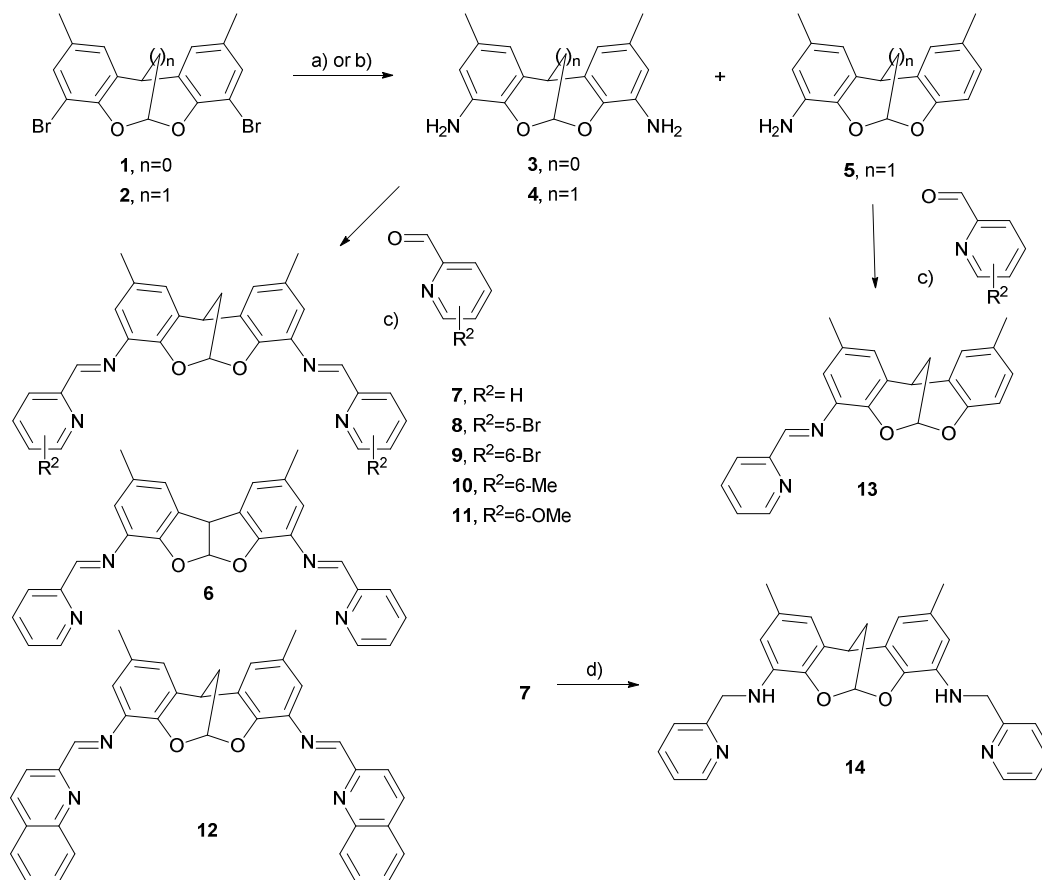
25 **Fig. 2** Desired and found coordination for BFBF and DBDOC derivatives.

Compounds **1** and **2** were prepared as reported previously.^{20,57,58} Firstly the synthesis of compounds **3** and **4** was attempted *via*
 30 nitration and further reduction, as for SPANamine.⁵⁹ The reaction was carried out under acidic conditions but decomposition of the backbone was observed due to acetal cleavage. This forced us to search for alternative routes such as cross-coupling reactions.

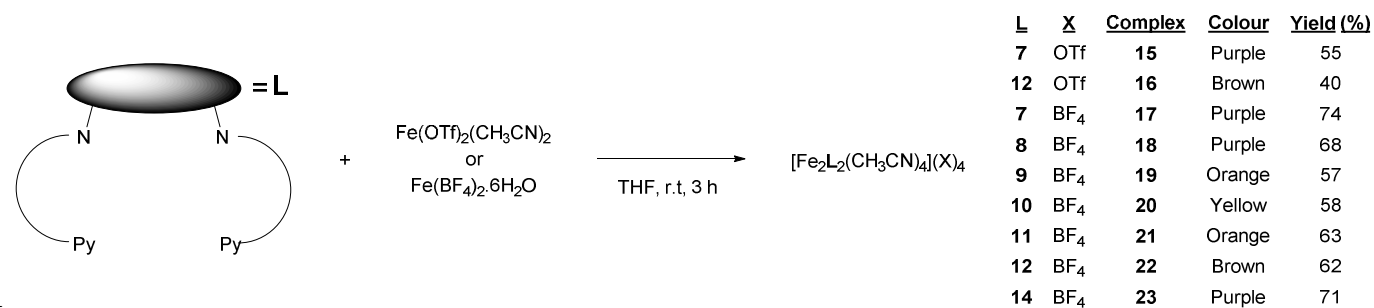
Cite this: DOI: 10.1039/c0xx00000x

www.rsc.org/xxxxxx

ARTICLE TYPE



Scheme 1 Reaction conditions: (a) NaN₃, proline, K₂CO₃, CuI, DMSO, 100 °C, 16h; (b) NH₃, Cu₂O, ethylene glycol, 110 °C, 3 d; (c) MgSO₄, THF, r.t., 16 h; (d) DIBAL-H, THF, r.t., 4 h.



Scheme 2 Synthesis of iron complexes with different tetranuclear ligands. Ligand s: **15**, **17-21** iminopyridine derivatives; **16** and **22** iminoquinoline and **23** aminopyridine

Our first approach was to synthesise the tetradentate ligands from **1** and **2** and several diamines *via* Buchwald–Hartwig coupling, but the reaction was not selective and a mixture of products was obtained, which included monosubstituted derivatives and products derived from reduction of the bromides. Cross coupling

with benzylamine also led to mixtures. Similar problems were observed when we attempted to use the Ullmann reaction for these compounds. A general scheme of the attempted reactions is shown at the supporting information. Finally intermediates **3** and **4** were prepared using NaN₃ as nitrogen source.⁶⁰ In view of the

potential explosion danger of intermediate azides and the high temperature needed, the reactions were carried on a small scale (below 150 mg). Multigram scale synthesis was feasible for **4** for which ammonia was used as nitrogen source. Product **5** was isolated as a by-product in this reaction. These intermediates **3-5** were really air-stable, since it was possible to use them even few months later the synthesis without further purification.

Finally the Schiff base condensation of the backbones with a wide variety of pyridine aldehyde derivatives and quinoline aldehyde led the formation of tetradentate nitrogen ligands in moderate to high yields (55–95%).

In order to improve the stability of the ligands, the final modification involves reduction of the imine function to yield the more stable aminopyridine derivatives. Compound **14** was isolated in 90% yield with the use of DIBAL-H as reducing agent. All compounds and intermediates **3-14** were characterized by NMR spectroscopy, elemental analysis and mass spectrometry.

Coordination chemistry studies

The synthesis and characterization of molecular complexes of metal DBDOC tetradentate derivatives was considered interesting and preliminary experiments were carried out in order to check if the desired dinuclear complexes were synthetically accessible.

All attempts to synthesize dinuclear MX_2M with bridging X ligands (X= halide, hydroxide, acetate) failed. Thus we turned to metal precursors with weakly coordinating anions.

Firstly the reactivity of **7** with iron(II) triflate was explored at a ligand:metal ratio of 1:2 which gave a deep purple solution in THF. After work-up, an excess of metal precursor was recovered and the MS of the sample indicated the formation of a product with a ligand:metal ratio of 1:1. With this information in hand it was decided to repeat the reaction changing the ligand and metal proportion from 1:2 to 1:1 (Scheme 2). With this procedure complex **15** was synthesized in moderate yields 55%. Crystals of compound **15** were grown from $\text{CH}_3\text{CN}:\text{Et}_2\text{O}$

in which a large intramolecular Fe–Fe distance of 9.273 Å is apparent. This large distance was attributed to the structure of the ligand; lack of bridging anions and the electrostatic repulsion between the iron centres and the lack of bridging anionic ligands.

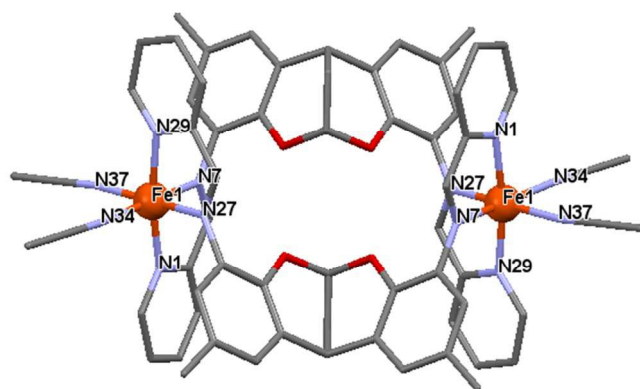
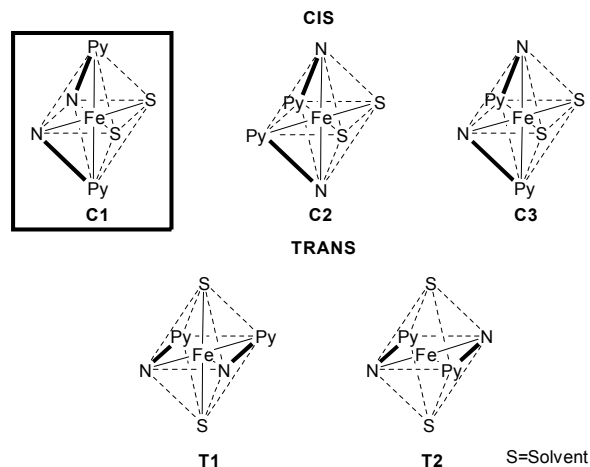


Fig. 3 The structure of the C_1 -symmetric cation present in the crystal of **15**.

The iron centres showed an octahedral geometry with angles around 90° and short N–Fe distances, shorter than 2 Å, indicative

of low spin complexes.⁶¹ Several isomers could be formed regarding the presence of bidentate imine ligands which coordinate to iron centres.⁶² Complex **15** has a C_{2h} symmetry with the pyridine donors *trans* to one another (Isomer C1 in Fig. 4)

Isomeric structures depending on coordination of ligand



Isomeric structures depending on the backbone

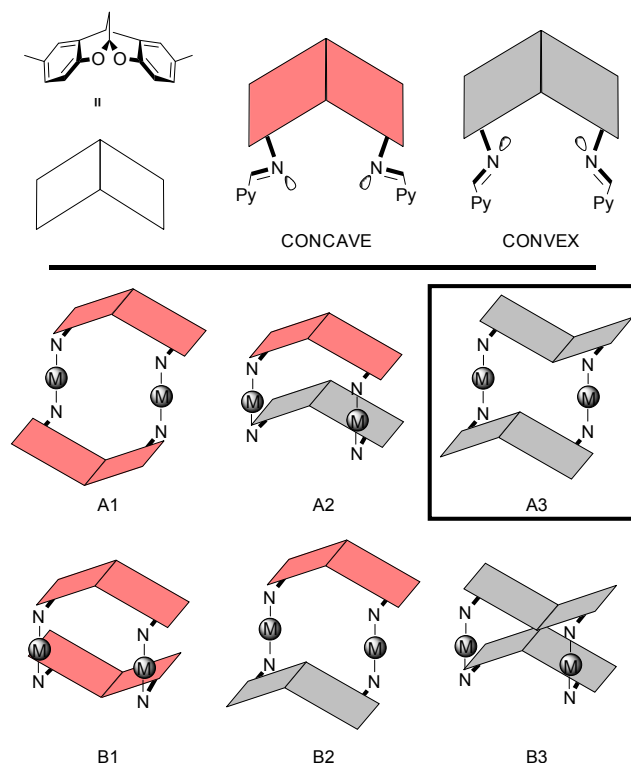


Fig. 4 Isomeric geometries for bidentate Fe diiminopyridine and isomeric face-to-face bimetallic complexes that may form with C_s symmetric ligands derived from DBDOC; three different conformers of each isomer A and B have been depicted, depending on the side (concave or convex) exposed to the metal centres. All determined structures present A3 geometry

Different arrangements of the DBDOC moiety can be expected as outlined before for related phosphine complexes of rhodium.²⁰ The isomers are summarized in Fig. 4, for the previous synthesized Rh-P complexes are known *A1* and *A3* geometry. In our case, we observed an *A3* geometry for compound **15**. The formation of this structure could be assisted by the formation of 4 π - π stacking interactions, with a distance between arene and pyridine of adjacent backbones of 3.9 Å (intramolecular) and 4.5 Å (intermolecular).^{63,64}

Once the reaction was optimized, the synthesis of new dinuclear complexes with tetradentate ligands was explored. Several iron complexes were prepared with the available BFBF and DBDOC derived tetradentate iminopyridine ligands. The reaction conditions and the synthesized complexes are summarized in Scheme 2.

Crystals of the complexes **15**, **16**, **18**, **19**, **20**, and **23** suitable for X-ray diffraction were obtained. The structures for complexes **16**, **18**, and **19** are shown in Fig. 5, the other structures can be found in the supporting information. The unit cell for compound **16** present three independent C_1 -symmetric complexes **16-A**, **16-B** and **16-C**; in the case of complex, **18** were observed two units **18-A** and **18-B**. Analysis of these structures revealed the same arrangement for these complexes; the iron atoms have an octahedral environment and the isomer formed has C_{2h} symmetry.

As regards the disposition of the DBDOC backbones, in all cases we observed the *A3* isomer. Moderate steric hindrance and electronic variations in the ligand did not affect the selectivity of the isomers formed.

The geometry of the iron (II) complexes was octahedral in all cases. However the spin of the complexes depend on the substituent in position 6. The low spin complexes do not have substituents at 6 and the N-Fe distance is around 2 Å as is observed literature in for these type of complexes.^{65,66} In contrast, 6-substituted complexes present high spin and the distance N-Fe is close to 2.2 Å. To be low spin the distance should be less than 2 Å which is prevented by the steric hindrance of the substituents. When there are substituents in *ortho* position of the pyridine nitrogen atom, we observe slightly distorted octahedrons, which was attributed to a steric effect. The distortion reduces the ligand field splitting and lowers the symmetry of the orbitals thus promoting the formation of high-spin compounds. If the substituent is in a *meta* position, low-spin complexes were obtained, as no distortion of the geometry takes place. A low-spin complex was also formed when aminopyridine derivatives were used (complex **23**) and quasi octahedral symmetry is observed in this complex. In Table 1 selected distances of the complexes are summarized

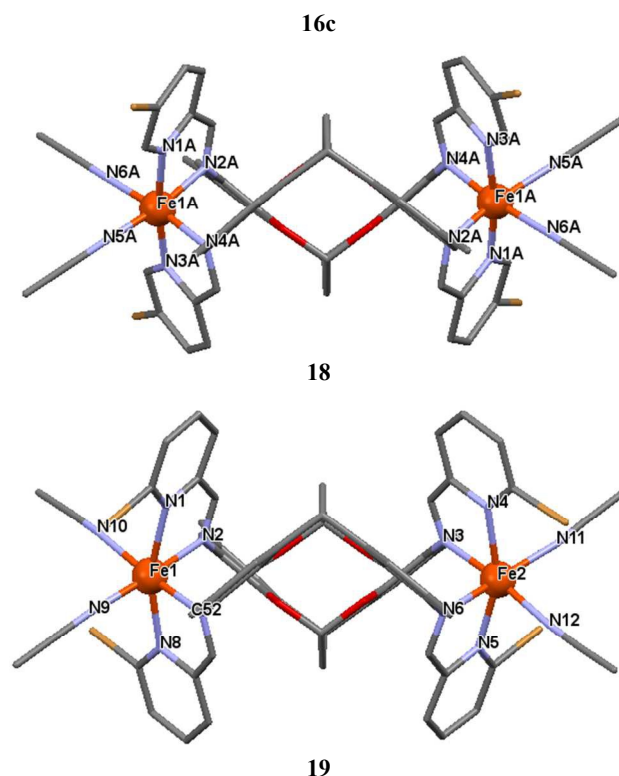
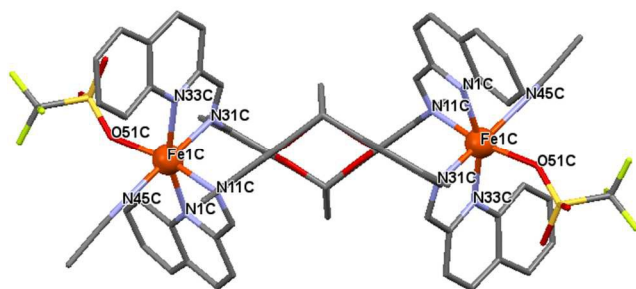


Fig. 5. The structure of cations present in the crystal of **16**, **18** and **19**. The symmetry for the complexes is C_1 for **16** and **18** and C_1 for **19**.

Table 1 Selected bond distances in Å for different X-ray structures of synthesized ligands.

Complex	Bond Distance(Å)			
	Fe-Fe	Fe-Py	Fe-Im	Fe-NCMe
15	9.2726(7)	1.9726(19)	1.9573(18)	1.952(2)
		1.9728(19)	1.9651(19)	1.953(2)
16-A	9.7537(9)	2.214(3)	2.175(3)	2.068(16)
		2.217(3)	2.195(3)	
16-B	10.0568(9)	2.201(3)	2.178(3)	2.06(3)
		2.211(3)	2.208(3)	
16-C	9.8045(9)	2.207(3)	2.159(3)	2.214(3)
		2.213(3)	2.191(3)	
17	9.0917(12)	1.965(3)	1.956(3)	1.946(3)
		1.9695(19)	1.961(3)	1.948(3)
18-A	9.0288(11)	1.963(2)	1.957(2)	1.945(2)
		1.964(2)	1.966(2)	1.953(2)
18-B	8.9200(12)	1.969(2)	1.954(2)	1.945(2)
		1.978(2)	1.962(2)	1.949(3)
19	9.5698(13)	2.214(5)	2.182(5)	2.128(5)
		2.233(3)	2.194(5)	2.161(6)
20	9.6102(17)	2.166(6)	2.158(6)	2.110(7)
		2.181(6)	2.161(6)	2.151(8)
23	9.2241(10)	2.047(2)	2.126(3)	2.015(4)
		2.048(3)	2.149(3)	2.029(3)

The electronic and steric properties of the ligands and the type of anion used affect the Fe-Fe distance. Low spin complexes (**15**, **17**, **18** and **23**) give shorter Fe-Fe distances than the high spin complexes (**16**, **19-22**) and the nature of the anion causes slight differences (Table 1, **15** and **17**). Ortho pyridine substituents in iron(II) complexes of this type generate a weaker ligand field and generally result in high spin complexes, as seen here for

complexes **16** and **19-22**.^{65,66}

In order to obtain more information about the structure of dinuclear complexes with other metals the copper (II) complex was prepared for ligand **7**. Like the aforementioned iron complexes, complexes with a metal:ligand ratio of 1:1 were formed. Crystals of **24** suitable for X-ray analysis were obtained from MeOH/Et₂O (Fig. 6). Two different structures were found in the unit cell, differentiated only by the coordination of MeOH (**24-A**) or OTf (**24-B**) in the equatorial position. Both species have an *A3* disposition of the DBDOC backbones. The geometry of copper is a distorted trigonal bipyramid.

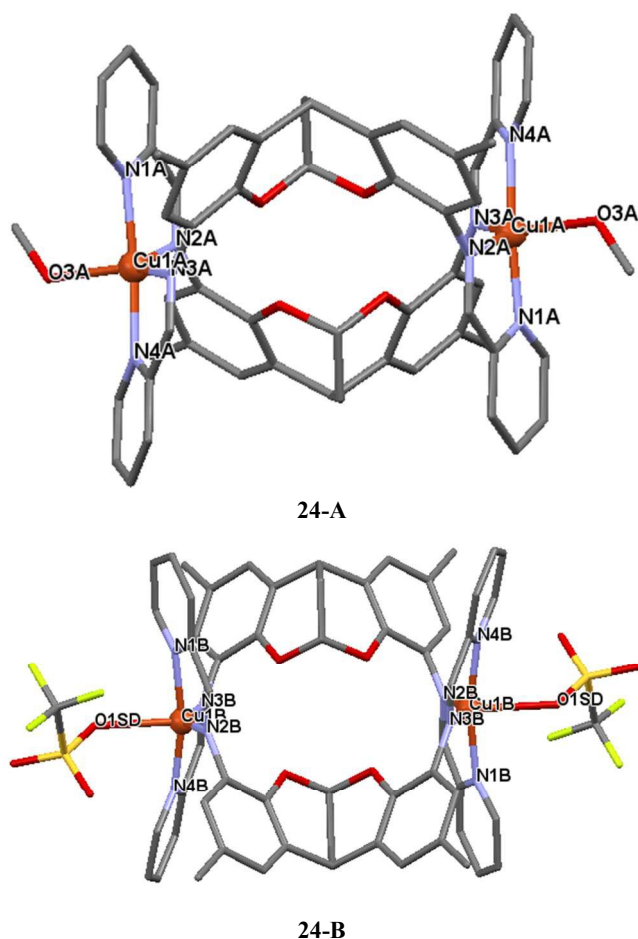


Fig. 6 The structure of the C₂-symmetric cations present in the crystal of **24**.

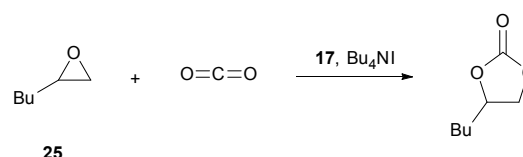
Some of the relevant bond lengths of complex **24** are summarized in Table 2. Of particular interest are the Cu–Cu distances. When the external equatorial position is occupied by anionic triflate, a smaller Cu–Cu distance is observed. The smaller difference is attributed to a decrease in electrostatic repulsion between the metals, as the overall positive charge for the Cu centre is +1, compared to +2 for the methanol complex. It can be seen that the iron complexes have longer M–M distances (9–10 Å) than the copper complexes, probably due to the different geometry at the metal centres.

Table 2 Selected bond distances in Å for different X-ray structures of complex **24**.

Complex	Bond Distance(Å)			
	Cu–Cu	Cu–Py	Cu–Im	Cu–O
24-A	8.2782(8)	1.984(2)	1.991(2)	2.1732(18)
24-B	7.6285(7)	1.984(2)	1.9949(19)	2.433(2)

Catalysis experiments

The iron complexes **17–23** were investigated as catalysts for the ring expansion of epoxides with carbon dioxide. Mononuclear and dinuclear complexes were tested as catalysts in this reaction in order to know if there is a cooperative effect of the metal centres in the dinuclear complexes causing a higher catalytic activity. The reaction is depicted in Scheme 3.



Scheme 3 Ring expansion of **25** with CO₂ promoted by iron complex **17**.

Firstly the results of the optimization of the temperature and pressure of the reaction are summarized in Fig. 7. The optimization was performed working below 85 °C to minimise the metal-free, ammonium-salt catalysed reaction as is known that ammonium quaternary salts can catalyze the ring expansion of epoxides with carbon dioxide.^{67–70} An increase of the yield was observed when the temperature was raised from 30 to 65 °C. When the pressure was kept constant at 10 bar, the highest yield observed was 55%. Raising the pressure led to higher activity of compound **17** as it observed in Fig. 7. According to literature, the rate determining step, should be the CO₂ insertion or ring closing step.⁷¹

P and T optimization

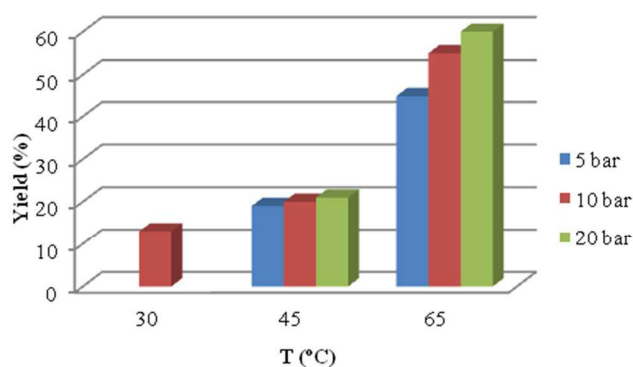


Fig. 7 P and T optimization in ring expansion of **25** with CO₂. Reaction conditions: 0.8 mmol substrate **25**, 1.25 mol% catalyst **17**, 1:2 Fe:Bu₄NI, in 2 mL of MEK. Yield determined by GC using mesitylene as internal standard.

The results of screening various co-catalysts are summarized in Table 3. In the first instance, the importance of complex:co-catalyst ratio was investigated. It was discovered that an iron:co-

catalyst ratio of 1:2 was required for an active system, and this was attributed to the coordination of iodide to the iron (II) centre due to the coordination to the metal as it was observed a change of color. The nature of the anion (entry 1, 3, and 4) was also found to have an important role. The best yields were obtained with iodide, and this can be attributed to its high nucleophilicity and group leaving ability compared to other halides which enhance both the ring opening and ring closing catalytic steps.⁷¹

Table 3 Co-catalyst screening in ring expansion of **25** with CO₂.

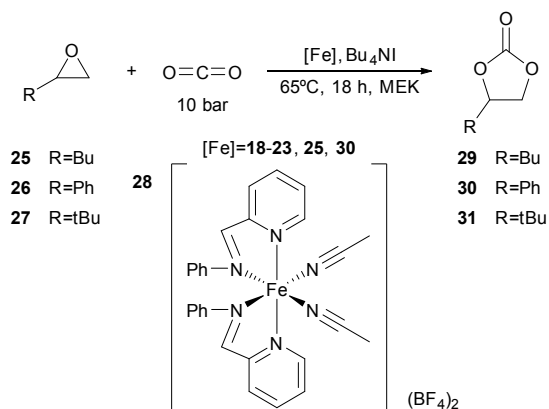
Entry	Co-catalyst	Yield ^a (%)
1	Bu ₄ NI	58
2 ^b	Bu ₄ NI	0
3	Bu ₄ NBr	44
4	Bu ₄ NCl	10
5	Me ₄ NI	10
6	Oct ₄ NBr	55
7	DMAP	1

0.8 mmol substrate, catalyst 2.5 mol %, pCO₂ = 10 bar, 18h, 65 °C, 1:2 Fe:co-catalyst, in 2 mL of MEK. ^a Chemical yield determined by GC using mesitylene as internal standard. ^b 1:1 Fe:co-catalyst.

Larger cations were also found to improve the yield (entries 1 vs 5 and 3 vs 6). The use of a neutral nucleophile instead of an anionic one dramatically reduced the reactivity and only 1% yield was observed with DMAP (entry 7). The results of this screening revealed that the best co-catalyst for iron complexes is tetrabutylammonium iodide with a 1:2 iron:iodide ratio.

The poor solubility of complex **17** limits the solvent scope to polar solvents and the best solvent proved to be methyl ethyl ketone giving yields of up to 60%. Acetonitrile and dimethoxyethane were also reasonable solvents, giving yields, above 50%. Methanol and acetone were the worst solvents giving yields of only 23% and 4% respectively. In light of this optimization, MEK was chosen as solvent for this transformation.

Once the reaction conditions were optimized, different iron complexes were screened as prospective catalysts (Scheme 4).



Scheme 4 Cyclic carbonate formation promoted by iron complexes.

The catalytic transformation of several epoxides using iron dinuclear complexes with different steric and electronic

properties in the pyridine moiety are summarized in Fig. 8. The transformation of **25** was initially targeted as a test reaction. The best catalyst for this substrate proved to be complex **17**, giving the expected cyclic carbonate **29** in 58 % yield. It was noted that electron donating substituents in the *ortho*-position led to a less active system and this is proposed to be the result of a reduction of the Lewis acidity of these complexes. This notion is supported by the fact that electron withdrawing groups in the *ortho*-position, bromine for example, gave higher yields.

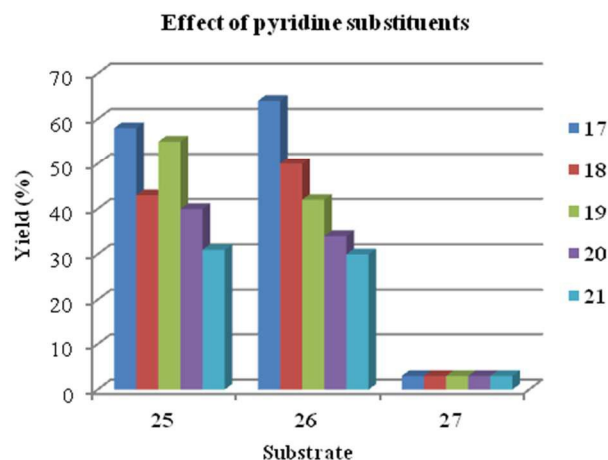


Fig. 8 Substrate and catalyst screening for catalytic formation of cyclic carbonates. Reaction conditions: 0.8 mmol substrate, 1.25 mol % catalyst, 18h, 65 °C, 1:2 Fe:Bu₄NI, in 2 mL of MEK. Chemical yield determined by GC using mesitylene as internal standard.

As in the case of **25**, the formation of the corresponding cyclic carbonate from styrene oxide, **26** followed the same trend. The best results were obtained with complex **17** as catalyst, followed by **18** and **19** with EWD groups. When epoxide **27** was used as substrate, similar very low conversions – above 3% – were observed for all the catalyst systems. This was attributed to the lack of coordination of the epoxide to the metal due to steric reasons. The low conversions observed are attributed to metal-free reactions catalysed by the ammonium salt.

The reactivity of the previously used epoxide were explored with different iron catalysts bearing aminopyridine coordinating groups, iminoquinoline instead of iminopyridine and mononuclear iminopyridine iron complexes. The results of these studies are summarized in Fig. 9.

The yield was comparable between **17**, **23**, and **28** when substrate **25** was used. If we compare **17** and **28** we can disregard any cooperative effect between the iron nuclei and they act as single monomeric units. Lower yields were obtained when the more crowded complex **22** was used.

When the substrate was changed to **26** lower yields were obtained with **22**, **23** and **28**. The best catalyst was found to be **17**. As we previously described, yields diminished when bulkier R substituents are present in the epoxide substrate.

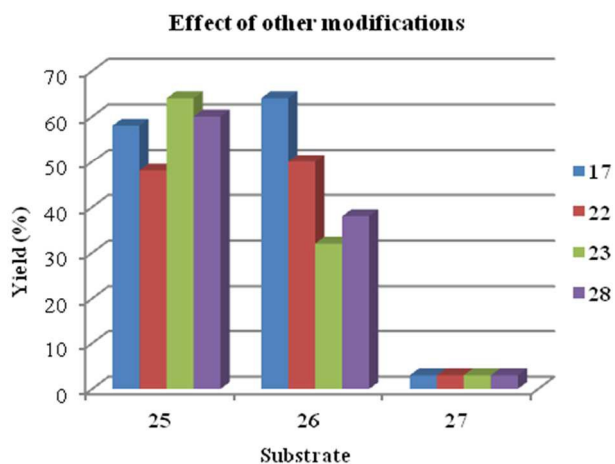


Fig. 9 Substrate and catalyst screening for catalytic formation of cyclic carbonates. Reaction conditions: 0.8 mmol substrate, 1.25 mol % catalyst, 18h, 65 °C, 1:2 Fe:Bu₄NI, in 2 mL of MEK. Chemical yield determined by GC using mesitylene as internal standard.

Conclusions

A family of dinuclear metal complexes where two DBDOC ligands act as a bridge were prepared for Fe and Cu. The iron complexes assumed an octahedral geometry with a cis coordination of the acetonitrile ligands where the DBDOC or act as a bridge ligand. Non substituted-pyridine ligands promoted the formation of low-spin diiron complexes with longer Fe–Fe distances. *Ortho* substituents deformed the octahedral and favoured the formation of high-spin complexes. In contrast a distorted trigonal bipyramidal geometry was observed in the case of a Cu(II) complex. In the X-ray structure two different compounds were observed which differ in the additional MeOH or TfO ligands in the equatorial face. The nature of the ligands has an influence on the Cu–Cu distance, being longer when neutral MeOH is acting as the ligand.

The new complexes, when tested in catalytic ring expansion of epoxides with carbon dioxide, presented moderate yields. Conversions were affected by the steric properties of the epoxides and the steric and electronic properties of the complex. In none of the cases we observed a cooperative effect of the iron nuclei in this catalytic transformation. Among all the catalyst tested in this report, the best catalyst for this reaction was complex **17**. The epoxides are converted under mild conditions in moderate yields which are comparable to known Fe(II) catalysts applied in this reaction.

Experimental

Unless otherwise stated, all reactions were performed using standard vacuum-line and Schlenk techniques under nitrogen atmosphere. All reagents were purchased from Sigma-Aldrich, solvents as HPLC grade and dried with an SPS system of ITC-inc. Reagents were used as commercially available. NMR spectra unless otherwise stated were recorded at the following frequencies: 400.13 MHz (¹H) and 100.63 MHz (¹³C) NMR spectra were recorded using broad band decoupling. Chemical shifts of ¹H and ¹³C NMR spectra are reported in ppm downfield from TMS, used as internal standard. Signals are quoted as s

(singlet), d (doublet), t (triplet), m (multiplet), b (broad)). Gas chromatograph analyses were run on a Hewlett-Packard HP 5890A instrument (split/splitless injector, J&W Scientific, IA, 25 m column, internal diameter 0.25 mm, film thickness 0.33 μm, carrier gas: He, F.I.D. detector) equipped with a Hewlett-Packard HP3396 series II integrator. The CG-MS are done in HP 6890 Series GC System coupled to HP 5973 Mass Selective Detector, with automatic injector HP 7683 Series Injector. The column is HP 5MS (30 m x 0.25 mm, and 0.25 film thickness μm). High pressure amination experiments were performed in Berghof Stainless Steel SS316 reactors (25 and 40 ml) equipped with a PTFE liner, magnetic stirring and heating jacket or in a Baskerville and Lindsay LTD. 6821 (20 ml) equipped with magnetic stirring. High pressure catalytic experiments were performed in a semiautomatic autoclave (AMTEC, Slurry phase reactor, SPR16) equipped with 16 stainless steel 15 mL reactors. All reactors were connected via a valve system with the gas supply and were equipped with individually adjustable stirring and heating.

2,9-dimethyl-5a,10b-dihydrobenzofuro[2,3-b]benzofuran-4,7-diamine, 3. A Schlenk tube was charge with proline (1.30 mmol), NaN₃ (130 mg, 2.00 mmol), CuI (190 mg, 1.0 mmol), and **1** (397 mg, 1.0 mmol). Degassed DMSO (2.0 mL) was added while flushing with argon. The flask was then placed in an oil bath maintained at 100 °C. The solution turned from dark red to dark brown over the course of the reaction. After completion of the reaction as judged by TLC, the dark solution was cooled and quenched by the addition of saturated aqueous NH₄Cl (3 mL) and EtOAc (2 mL). This biphasic mixture was stirred at r.t. for 1 h. The resulting dark green solution was filtered through a pad of Celite, which was subsequently washed with EtOAc and water. The filtrate was extracted with EtOAc and washed with brine. Finally the organic phases were combined, dried with MgSO₄, filtered, and concentrated. The solid was loaded on a neutralized silica gel column and eluted with DCM to afford pure compound **3** as off-white powder. In view of the potential explosion danger of intermediate azides and the high temperature needed, the reactions were carried on a small scale (below 150 mg) Yield: 37%. ¹H NMR (500 MHz, DMSO-*d*₆) δ = 6.88 (d, *J* = 6.7 Hz, 1H, C–H), 6.48 (d, *J* = 1.6 Hz, 2H, Ar–H), 6.30 (d, *J* = 1.5 Hz, 2H, Ar–H), 4.91 (d, *J* = 6.7 Hz, 1H, C–H), 4.70 (b, 4H, N–H₂), 2.13 (s, 6H, C–H₃). ¹³C NMR (126 MHz, DMSO-*d*₆) δ = 142.41, 132.26, 131.36, 127.58, 115.11, 112.43, 51.47. ESI⁺: calcd. for C₁₆H₁₆N₂NaO₂ [M⁺] 291.11; found 291.1

2,10-dimethyl-12H-6,12-methanodibenzo[d,g][1,3]dioxocine-4,8-diamine, 4. A 40 mL stainless steel reactor was charged with **2** (6 mmol), copper oxide (I) (2 mmol), and 12 mL of 1,2-ethanediol. The mixture was cooled in an acetone/CO₂ bath, while 12 mL of ammonia were condensed with an acetone/CO₂ bath. The liquid ammonia was added to the solid solution of 1,2-ethanediol. The reactor was closed and temperature was increased to 110°C. Reaction was stopped after 3 days. Water (200 mL) and DCM (200 mL) were added to the dark blue solution. The aqueous phase is extracted with DCM (3x200 mL). The organic phases were combined and cleaned with 100 mL of brine. Finally the organic phase was dried with MgSO₄, filtered, and dried. The

yellowish solid was loaded on a silica gel column and eluted with DCM to afford pure compound as off-white powder (third fraction). Yield: 90%. ^1H NMR (400 MHz, Chloroform-*d*) δ = 6.45 (s, 2H, Ar-H), 6.41 – 6.34 (m, 2H, Ar-H), 6.25 (q, J = 2.0 Hz, 1H, C-H), 3.79 (td, J = 3.0, 1.4 Hz, 1H, C-H), 2.23 (dd, J = 3.1, 2.1 Hz, 2H, C-H₂), 2.21 (s, 6H, C-H₃). ^{13}C NMR (101 MHz, Chloroform-*d*) δ = 136.58, 134.46, 130.75, 126.44, 117.40, 114.88, 91.97, 31.32, 25.98, 20.78. ESI⁺: calcd. for C₁₇H₁₈N₂NaO₂ [M⁺] 315.13; found 305.1.

2,10-dimethyl-12H-6,12-methanodibenzo[d,g][1,3]dioxocin-4-amine, 5, was recovered as off-white powder from a silica gel column performed in the synthesis of **4** (second fraction). ^1H NMR (300 MHz, Chloroform-*d*) δ = 7.03 – 6.98 (m, 1H, Ar-H), 6.90 (ddd, J = 8.3, 2.1, 0.8 Hz, 1H, Ar-H), 6.79 (d, J = 8.3 Hz, 1H, Ar-H), 6.45 (dt, J = 2.0, 0.7 Hz, 1H, Ar-H), 6.38 (dd, J = 2.0, 0.7 Hz, 1H, Ar-H), 6.18 (td, J = 2.2, 1.6 Hz, 1H, C-H), 3.83 (q, J = 2.2, 1.5 Hz, 1H, C-H), 3.73 (b, 2H, N-H₂), 2.27 (s, 3H, C-H₃), 2.23 (dd, J = 3.0, 2.2 Hz, 2H, C-H₂), 2.20 (s, 3H, C-H₃). ^{13}C NMR (126 MHz, Chloroform-*d*) δ = 148.72, 136.46, 134.69, 130.85, 130.53, 128.48, 127.96, 126.46, 117.09, 116.10, 114.84, 92.09, 31.54, 25.85, 20.77, 20.54. ESI⁺: calcd. for C₁₇H₁₇NNaO₂ [M⁺] 290.12; found 290.1.

(N⁴E,N⁷E)-2,9-dimethyl-N⁴,N⁷-bis(pyridin-2-ylmethylene)-5a,10b-dihydrobenzofuro[2,3-b]benzofuran-4,7-diamine, 6. A Schlenk tube was charged with **3**, (0.5 mmol), picolinaldehyde (1 mmol) and 9 mL of THF. Then MgSO₄ was added. The reaction was stirred for 16 hours. Filtration was done and the solution evaporate yielding a yellow solid. Yield: 55% ^1H NMR (500 MHz, Chloroform-*d*) δ = 8.90 (s, 2H, N=C-H), 8.75 – 8.69 (m, 2H, Ar-H), 8.30 – 8.24 (m, 2H, Ar-H), 7.84 – 7.77 (m, 2H, Ar-H), 7.36 (ddd, J = 7.4, 4.9, 1.3 Hz, 2H, Ar-H), 7.15 – 7.13 (m, 2H, Ar-H), 7.06 (d, J = 6.8 Hz, 1H, C-H), 7.01 (d, J = 1.9 Hz, 2H, Ar-H), 5.06 (d, J = 6.8 Hz, 1H, C-H), 2.37 (s, 6H, C-H₃). ^{13}C NMR (126 MHz, Chloroform-*d*) δ = 162.38, 149.55, 148.56, 136.52, 132.40, 128.57, 125.03, 123.10, 122.71, 121.88, 113.55, 50.26, 20.87, 1.02. ESI⁺: calcd. for C₂₈H₂₂N₄O₄Na⁺ [M⁺] 469.16; found 469.1.

(N⁴E,N⁸E)-2,10-dimethyl-N⁴,N⁸-bis(pyridin-2-ylmethylene)-12H-6,12-methanodibenzo[d,g][1,3]dioxocine-4,8-diamine, 7. In a Schlenk tube was charged with **4**, (0.5 mmol), picolinaldehyde (1 mmol) and 9 mL of THF. Then MgSO₄ was added. The reaction was stirred for 16 hours. Filtration was done and the solution evaporate yielding a yellow solid. Yield: 95%. ^1H NMR (400 MHz, Chloroform-*d*) δ = 8.72-69 (m, 2H, Ar-H), 8.60 (s, 2H, N=C-H), 8.25 (d, J = 7.9 Hz, 2H, Ar-H), 7.85 (td, J = 7.6, 1.3 Hz, 2H, Ar-H) 7.40 (ddd, J = 7.4, 4.8, 1.2 Hz, 2H, Ar-H), 7.01 (d, J = 1.7 Hz, 2H, Ar-H), 6.80 (d, J = 1.5 Hz, 2H, Ar-H), 6.30 (d, J = 1.7 Hz, 1H, C-H), 4.05 (d, J = 1.5 Hz, 1H, C-H), 2.38-35 (m, 2H, C-H₂), 2.34 (s, 6H, C-H₃). ^{13}C NMR (75 MHz, Chloroform-*d*) δ = 161.87, 154.8, 149.59, 141.67, 139.38, 136.51, 131.08, 127.48, 125.88, 125.08, 121.36, 119.36, 92.31, 31.77, 25.20, 20.27. C₂₉H₂₄N₄O₂ (460.19): calcd. C, 75.63; H, 5.25; found C, 75.39; H, 5.30. ESI⁺: calcd. for C₂₉H₂₄N₄O₂ [M⁺] 460; found 460.

(N⁴E,N⁸E)-2,10-dimethyl-N⁴,N⁸-bis((5-bromopyridin-2-yl)methylene)-2,10-dimethyl-12H-6,12-methanodibenzo[d,g][1,3]dioxocine-4,8-diamine, 8. Compound **8** was prepared following the same procedure described above for compound **7**, but using 5-bromopicolinaldehyde as aldehyde. Compound was isolated as a yellow solid. Yield: 94%. ^1H NMR (500 MHz, Chloroform-*d*) δ = 8.75 (dd, J = 2.4, 0.8 Hz, 2H, Ar-H), 8.57 (d, J = 0.7 Hz, 2H, N=C-H), 8.17 (dd, J = 8.4, 0.8 Hz, 2H, Ar-H), 7.93 (ddd, J = 8.5, 2.4, 0.7 Hz, 2H, Ar-H), 6.98 (d, J = 2.1 Hz, 2H, Ar-H), 6.78 (dd, J = 2.1, 0.9 Hz, 2H, Ar-H), 6.36 (d, J = 1.8 Hz, 1H, C-H), 4.01 (d, J = 2.2 Hz, 1H, C-H), 2.32 (s, 8H, C-H₂ and C-H₃). ^{13}C NMR (126 MHz, Chloroform-*d*) δ = 160.62, 153.25, 150.62, 141.71, 139.23, 138.90, 130.97, 127.33, 126.27, 122.94, 122.59, 120.16, 92.29, 31.83, 25.19, 20.57. C₂₉H₂₂Br₂N₄O₂ (618.32): calcd. C, 56.33; H, 3.59; found C, 56.27; H, 4.01. ESI⁺: calcd. for C₂₉H₂₂Br₂N₄O₂Na⁺ [M⁺] 641.0; found 640.9

(N⁴E,N⁸E)-2,10-dimethyl-N⁴,N⁸-bis((6-bromopyridin-2-yl)methylene)-2,10-dimethyl-12H-6,12-methanodibenzo[d,g][1,3]dioxocine-4,8-diamine, 9. Compound **9** was prepared following the same procedure described above for compound **7**, but using 6-bromopicolinaldehyde as aldehyde. Compound was isolated as a yellow solid. Yield: 73%. ^1H NMR (500 MHz, Chloroform-*d*) δ = 8.60 (d, J = 0.7 Hz, 2H, N=C-H), 8.27 (dd, J = 7.7, 1.0 Hz, 2H, Ar-H), 7.67 (td, J = 7.7, 0.7 Hz, 2H, Ar-H), 7.55 (dd, J = 7.8, 0.9 Hz, 2H, Ar-H), 6.98 (dt, J = 2.1, 0.7 Hz, 2H, Ar-H), 6.80 (dd, J = 2.2, 0.8 Hz, 2H, Ar-H), 6.36 (d, J = 1.9 Hz, 1H, C-H), 4.01 (q, J = 2.6 Hz, 1H, C-H), 2.36 – 2.26 (m, 8H, C-H₂ and C-H₃). ^{13}C NMR (126 MHz, Chloroform-*d*) δ = 160.19, 156.00, 141.76, 141.55, 138.82, 138.52, 130.99, 129.39, 127.34, 126.45, 120.44, 92.26, 31.83, 25.16, 20.56, 1.03. C₂₉H₂₂Br₂N₄O₂ (618.32): calcd. C, 56.33; H, 3.59; found C, 55.12; H, 3.76. ESI⁺: calcd. for C₂₉H₂₂Br₂N₄O₂Na⁺ [M⁺] 641.0; found 640.9

(N⁴E,N⁸E)-2,10-dimethyl-N⁴,N⁸-bis(pyridin-2-ylmethylene)-12H-6,12-methanodibenzo[d,g][1,3]dioxocine-4,8-diamine, 10. Compound **10** was prepared following the same procedure described above for compound **7**, but using 6-methylpicolinaldehyde as aldehyde. Compound was isolated as a yellow solid. Yield: 70% ^1H NMR (500 MHz, Chloroform-*d*) δ = 8.58 (d, J = 0.6 Hz, 2H, N=C-H), 8.10 (d, J = 7.6 Hz, 2H, Ar-H), 7.69 (t, J = 7.8 Hz, 2H, Ar-H), 7.24 – 7.20 (m, 2H, Ar-H), 6.99 – 6.95 (m, 2H, Ar-H), 6.79 (dd, J = 2.2, 0.9 Hz, 2H, Ar-H), 6.38 (q, J = 2.0 Hz, 1H, C-H), 3.99 (q, J = 2.7 Hz, 1H, C-H), 2.63 (s, 6H, C-H₃), 2.33 – 2.30 (m, 8H, C-H₂ and C-H₃). ^{13}C NMR (126 MHz, Chloroform-*d*) δ = 162.07, 154.21, 141.75, 137.13, 136.70, 130.77, 125.86, 124.68, 119.99, 119.09, 119.05, 117.04, 92.10, 24.34, 20.56, 1.02. C₃₁H₂₈N₄O₂ (488.58): calcd. C, 76.21; H, 5.78; found C, 76.02; H, 5.91. ESI⁺: calcd. for C₃₁H₂₈N₄O₂Na⁺ [M⁺] 511.21; found 511.1.

(N⁴E,N⁸E)-2,10-dimethyl-N⁴,N⁸-bis((6-methoxypyridin-2-yl)methylene)-2,10-dimethyl-12H-6,12-methanodibenzo[d,g][1,3]dioxocine-4,8-diamine, 11. Compound **11** was prepared following the same procedure described above for compound **7**, but using 6-methoxypicolinaldehyde as aldehyde. Compound was isolated as a yellow solid. Yield: 85%. ^1H NMR (500 MHz,

Chloroform-*d*) δ = 8.46 (d, J = 2.1 Hz, 2H, N=C-H), 7.85 (dd, J = 7.3, 0.9 Hz, 2H, Ar-H), 7.67 (ddd, J = 8.0, 7.4, 0.7 Hz, 2H, Ar-H), 6.96 (d, J = 2.1 Hz, 2H, Ar-H), 6.81 (dd, J = 8.2, 0.8 Hz, 2H, Ar-H), 6.76 (dd, J = 2.1, 0.8 Hz, 2H, Ar-H), 6.39 – 6.37 (m, 5 1H, C-H), 3.99 (s, 7H, C-H and C-H₃), 2.32 (s, 8H, C-H₂ and C-H₃). ¹³C NMR (126 MHz, Chloroform-*d*) δ = 163.88, 161.88, 152.26, 141.76, 139.61, 138.83, 130.73, 127.25, 125.77, 119.77, 115.00, 112.56, 92.27, 53.43, 31.91, 25.24, 20.59. C₃₁H₂₈N₄O₄ (488.58): calcd. C, 71.52; H, 5.42; found C, 70.64; H, 5.63. ESI⁺: 10 calcd. for C₃₁H₂₈N₄O₄Na⁺ [M⁺] 543.20; found 543.1.

(N⁴E,N⁸E)-2,10-dimethyl-N⁴,N⁸-bis(quinolin-2-ylmethylene)-12H-6,12-methanodibenzo[d,g][1,3]dioxocine-4,8-diamine, 12.

Compound **12** was prepared following the same procedure 15 described above for compound **7**, but using quinoline-2-carbaldehyde as aldehyde. Compound was isolated as a yellow solid. Yield: 80 %. ¹H NMR (400 MHz, Chloroform-*d*) δ = 8.72 (s, 2H, N=C-H), 8.34 (d, J = 8.5 Hz, 2H, Ar-H), 8.25 (d, J = 8.6 Hz, 2H, Ar-H), 8.10 (t, J = 8.7 Hz, 2H, Ar-H), 7.88 (d, J = 7.5 Hz, 2H, Ar-H), 7.74 (ddd, J = 8.4, 6.9 1.4 Hz, 2H, Ar-H), 7.59 (ddd, J = 8.0, 6.9 1.0 Hz, 2H, Ar-H), 7.01 (d, J = 1.7 Hz, 2H, Ar-H), 6.84 (d, J = 1.7 Hz, 2H, Ar-H), 6.32 (d, J = 1.7 Hz, 1H, C-H), 4.04 (d, J = 1.5 Hz, 1H, C-H), 2.36-33 (m, 2H, C-H₂), 2.31 (s, 25 6H, C-H₃). ¹³C NMR (75 MHz, Chloroform-*d*) δ = 162.58, 155.59, 148.59, 142.39, 139.76, 137.07, 131.72, 130.29, 129.70, 126.46, 128.32, 128.17, 128.13, 126.77, 120.10, 119.05, 92.97, 32.35, 26.13, 20.85. C₃₇H₂₈N₄O₂ (560.22): calcd. C, 79.27; H, 5.03; found C, 78.39; H, 5.29. EI⁺: calcd. for C₃₇H₂₈N₄O₂ [M⁺] 560; found 560.

(E)-2,10-dimethyl-N-(pyridin-2-ylmethylene)-12H-6,12-methanodibenzo[d,g][1,3]dioxocin-4-amine, 13.

Compound **13** was prepared following the same procedure described above for 35 compound **7**, but using 2,10-dimethyl-12H-6,12-methanodibenzo[d,g][1,3]dioxocin-4-amine as amine. Compound was isolated as a yellow solid. Yield: 90%. ¹H NMR (500 MHz, Chloroform-*d*) δ = 8.71 (ddd, J = 4.8, 1.7, 0.9 Hz, 1H, Ar-H), 8.61 (d, J = 0.7 Hz, 1H), 8.30 (dt, J = 7.9, 1.1 Hz, 1H, N=C-H), 7.85 – 7.78 (m, 1H, Ar-H), 7.37 (ddd, J = 7.5, 4.8, 1.2 Hz, 1H, Ar-H), 7.05 (dd, J = 2.2, 0.8 Hz, 1H, Ar-H), 6.96 – 6.90 (m, 2H, Ar-H), 6.82 (d, J = 8.1 Hz, 1H, Ar-H), 6.77 (dd, J = 2.1, 0.9 Hz, 1H, Ar-H), 6.26 (q, J = 2.1 Hz, 1H, C-H), 3.95 (q, J = 2.6 Hz, 1H, C-H), 2.32 – 2.29 (m, 6H, C-H₃), 2.29 – 2.25 (m, 2H, C-H₂). ¹³C NMR (126 MHz, Chloroform-*d*) δ = 161.91, 154.75, 45 149.52, 141.73, 139.31, 136.51, 130.82, 130.59, 128.66, 127.77, 127.55, 126.15, 125.95, 125.04, 121.93, 119.88, 116.39, 92.22, 31.84, 25.46, 20.57, 20.55. C₂₃H₂₀N₂O₂ (356.42): calcd. C, 77.51; H, 5.66; found C, 77.24; H, 5.85. ESI⁺: calcd. for C₂₃H₂₀N₂O₂Na⁺ [M⁺] 379.14; found 379.1.

Synthesis of 2,10-dimethyl-N⁴,N⁸-bis(pyridin-2-ylmethyl)-12H-6,12-methanodibenzo[d,g][1,3]dioxocine-4,8-diamine, 14.

Under inert conditons, a Schlenk tube was charged with 2 mL of diisobutylaluminum hydride (1M) and 7 mL of diethylether. Then 57 **7** was added (116 mg, 0.25 mmol). The reaction was stirred for 4 hours. Then 5 mL of water was added and the solution extracted with DCM (3x10 mL). The organic phase was dried over MgSO₄ anhydrous and evaporated yielding a white solid. Yield: 90%. ¹H

NMR (500 MHz, Chloroform-*d*) δ = 8.61 (ddd, J = 4.9, 1.8, 0.9 60 Hz, 2H, Ar-H), 7.65 (td, J = 7.7, 1.8 Hz, 2H, Ar-H), 7.38 (dt, J = 8.0, 1.0 Hz, 2H, Ar-H), 7.19 (ddd, J = 7.5, 4.9, 1.2 Hz, 2H, Ar-H), 6.43 (d, J = 1.9 Hz, 2H, Ar-H), 6.33 (q, J = 2.0 Hz, 1H, C-H), 6.21 (d, J = 1.9 Hz, 2H, Ar-H), 5.08 (s, 2H, N-H), 4.47 (s, 4H, C-H₂), 3.81 (q, J = 1.5 Hz, 1H, C-H), 2.26 (dd, J = 3.0, 2.1 65 Hz, 2H, C-H₂), 2.19 (s, 6H, C-H₃). ¹³C NMR (126 MHz, Chloroform-*d*) δ = 159.22, 149.36, 136.78, 136.57, 131.05, 125.80, 122.09, 121.57, 116.00, 110.23, 100.13, 92.16, 49.54, 31.45, 26.14, 21.29. C₂₉H₂₈N₄O₂ (464.56): calcd. C, 74.98; H, 6.08; found C, 73.97; H, 5.72. ESI⁺: calcd. for C₂₉H₂₈N₄O₂Na⁺ 70 [M⁺] 487.21; found 487.1.

Synthesis of Fe complexes with Fe(OTf)₂(CH₃CN)₂ as precursor.

A THF (2 mL) solution of ligand (0.1 mmol) was added to a stirring solution of Fe(OTf)₂(CH₃CN)₂ (0.1 mmol) in 75 THF (2 mL). The resulting solution was allowed to stir during 3h. Then 10 mL of dry diethyl ether were added and the suspension was filtered and dried. The resulting solid was washed 3 times with diethyl ether and dried under vacuum.

[Fe₂7₂(CH₃CN)₄](OTf)₄, 15. It was isolated as a purple complex. Yield: 55%. ¹H NMR (400 MHz, CD₃CN) δ = 10.50 (s), 9.68 (s), 7.31 (s), 6.35 (s), 6.06 (s), 5.15 (s), 3.67 (s), 3.45 (s), 3.25 (s), 1.30 (s), 1.15 (s), 0.91 (s). LSIMS⁺: calcd. for C₆₁H₄₈F₉Fe₂N₈O₁₃S₃⁺ [Fe₂(7)₂(OTf)₃] [M⁺] 1479.11; found 85 1479.

[Fe₂12₂(CH₃CN)₂(OTf)₂](OTf)₂, 16. It was isolated as a dark brown complex. Yield: 40% ¹H NMR (500 MHz, Acetonitrile-*d*₃) δ = 52.08 (d, J = 281.8 Hz), 24.52 (s), 10.12 – 9.39 (m), 8.10 90 (m), 6.35 (d, J = 73.9 Hz), 5.11 (s), 4.14 – 3.46 (m), -9.07 (s), -14.02 (s), -26.88 (s). LSIMS⁺: calcd. for C₄₀H₂₈F₉Fe₂N₄O₁₁S₃⁺ [Fe₂72(OTf)₃] [M⁺] 1119.54; found 1120.

Synthesis of Fe complexes with Fe(BF₄)₂·6H₂O as precursor.

A Schlenk tube was charged with Fe(BF₄)₂·6H₂O (34 mg, 0.1 mmol). Then 3 mL of dry THF and 0.1 mL of triethyl orthoformate (TEOF) (0.6 mmol) were added. The solution was stirred for 30 min and it became light purple. Ligand was added 95 (0.1 mmol) to the stirring solution. The resulting solution was allowed to stir during 3h. Then 10 mL of dry diethyl ether were added and the solution was filtered and dried. The resulting solid was clean 3 times with diethyl ether and dried under vacuum.

[Fe₂7₂(CH₃CN)₄](BF₄)₄, 17. 72 It was isolated as a purple 105 complex. Yield: 74% ¹H NMR (400 MHz, CD₃CN) δ = 10.50 (s), 9.68 (s), 7.31 (s), 6.35 (s), 6.06 (s), 5.15 (s), 3.67 (s), 3.45 (s), 3.25 (s), 1.30 (s), 1.15 (s), 0.91 (s). C₆₆H₆₀B₄F₁₆Fe₂N₁₂O₄·4H₂O (1616.41): calcd. C, 49.05; H, 4.24; found C, 48.81; H, 4.24.

[Fe₂8₂(CH₃CN)₄](BF₄)₄, 18. It was isolated as a purple complex. Yield: 68%. ¹H NMR (500 MHz, Acetonitrile-*d*₃) δ = 14.85 (bs), 12.21 (bs), 9.76 (s), 7.90 (s), 6.41 (m), 5.13 (s), 4.67 (s), 3.49 (s), 1.96 (s), 1.06 (s). C₆₆H₅₆B₄Br₄F₁₆Fe₂N₁₂O₄·4H₂O (1967.07): 115 calcd. C, 40.28; H, 3.48; found C, 40.78; H, 3.45.

[Fe₂9₂(CH₃CN)₄](BF₄)₄, **19**. It was isolated as an orange complex. Yield: 57%. ¹H NMR (500 MHz, Acetonitrile-*d*₃) δ = 10.24 – 9.90 (m), 8.22, (s), 8.11 – 7.72 (m), 7.49 – 7.21 (m), 7.01 (s), 6.35 (s), 4.68 (s), 4.17 (s), 3.16 (s), 2.29 (s), 1.26 (s). C₆₆H₅₆B₄Br₄F₁₆Fe₂N₁₂O₄·4H₂O (1967.07): calcd. C, 40.28; H, 3.48; found C, 40.85; H, 3.43.

[Fe₂10₂(CH₃CN)₄](BF₄)₄, **20**. It was isolated as a yellow complex. Yield: 58%. ¹H NMR (500 MHz, Acetonitrile-*d*₃) δ = 56.41 (b), 24.86 (b), 8.97 (s), 8.52 (s), 8.10 (d), 7.95 – 7.80 (m), 7.33 (s), 7.03 (s), 2.33 – 2.08 (m), -10.29 (b), -15.27 (b), -29.96 (b). C₇₀H₆₈B₄F₁₆Fe₂N₁₂O₄·4H₂O (1672.34): calcd. C, 50.27; H, 4.58; found C, 50.06; H, 4.59.

[Fe₂11₂(CH₃CN)₄](BF₄)₄, **21**. It was isolated as an orange complex. Yield: 63%. ¹H NMR (500 MHz, CD₃CN) δ = 75.31 (b), 53.10 (b), 22.31 (b), 9.83 (b), 9.17 (b), 7.89 (b), 7.35 (b), 6.35 (b), -3.02 (b), -7.79 (b), -13.05 (b), -21.85 (b). C₇₀H₆₈B₄F₁₆Fe₂N₁₂O₈·4H₂O (1736.34): calcd. C, 48.42; H, 4.41; found C, 48.58; H, 4.51.

[Fe₂12₂(CH₃CN)₄](BF₄)₄, **22**. It was isolated as a brown complex. Yield: 62%. ¹H NMR (500 MHz, Acetonitrile-*d*₃) δ = 52.08 (d), 24.52 (s), 10.12 – 9.39 (m), 8.10 (m), 6.35 (d), 5.11 (s), 4.14 – 3.46 (m), -9.07 (s), -14.02 (s), -26.88 (s). C₈₂H₆₈B₄F₁₆Fe₂N₁₂O₄·6H₂O (1816.46): calcd. C, 53.16; H, 4.35; found C, 53.18; H, 4.20.

[Fe₂14₂(CH₃CN)₄](BF₄)₄, **23**.⁷² It was isolated as an purple complex. Yield: 71%. ¹H NMR (500 MHz, CD₃CN) δ = 8.54 (s), 8.01 (s), 7.99(s), 7.92 (s), 6.57(s), 6.32 (s), 6.07(s), 4.76 (bs), 3.92 (s), 2.26 (s), 2.22 (s). C₆₆H₆₈B₄F₁₆Fe₂N₁₂O₄·4H₂O (1624.29): calcd. C, 48.80; H, 4.72; found C, 48.52; H, 4.62.

[Cu₂8₂(MeOH)₂](OTf)₂, **24**. A Schlenk tube was charged with Cu(OTf)₂ (185 mg, 0.5 mmol). The system was sealed with a septum. The flask was evacuated and backfilled with inert gas three times. Methanol was added (23 mL) and later compound **24** (231 mg, 0.5 mmol). The resulting solution was allowed to stir during 16h. Then 40 mL of dry diethyl ether were added and the solution was filtered and dried. The resulting solid was clean 3 times with diethyl ether and dried under vacuum. The brown solid was solubilized in MeOH and crystallized from slow diffusion of ether. Yield: 70%. C₆₄H₅₆Cu₂F₁₂N₈O₁₈S₄ (2327,87): calcd. C, 44.99; H, 3.30; found C, 44.04; H, 3.40. ESI⁺: calcd. for C₆₀H₅₄Cu₂N₈O₆²⁺ [Cu₂8₂(MeO)₂] [M⁺] 555.13; found 555.1

X-Ray structure determinations†

Single crystals of compounds **15**, **16**, **18**, **19**, **20**, and **23** by slow evaporation of Et₂O into a CH₃CN solution. Crystals of complex **24** were obtained by slow diffusion of Et₂O into MeOH. The measured crystals were prepared under inert conditions immersed in perfluoropolyether as protecting oil for manipulation.

Data collection: Crystal data for **15** and **16** were collect using an Oxford (Agilent) Diffraction Xcalibur 3 diffractometer. Crystal structure determinations for **18**, **19** and **20** were carried out using a Apex DUO diffractometer equipped with a Kappa 4-axis

goniometer, an APEX II 4K CCD area detector, a Microfocus Source E025 IuS using MoK_α radiation, Quazar MX multilayer Optics as monochromator and an Oxford Cryosystems low temperature device Cryostream 700 plus (*T* = -173 °C). Full-sphere data collection was used with ω and φ scans. Crystal structure determinations for **23** and **24** were carried out using a Bruker-Nonius diffractometer equipped with an APEX II 4K CCD area detector, a FR591 rotating anode with MoK_α radiation, Montel mirrors as monochromator, a Kappa 4-axis goniometer and an Oxford Cryosystems low temperature device Cryostream 700 plus (*T* = -173 °C).

Programs used Data collection Apex2 V. 1.0-22 (Bruker-Nonius 2004), data reduction Saint+Version 6.22 (Bruker-Nonius 2001) and absorption correction SADABS V. 2.10 (2003). For samples **15** and **15** the software package CrystAlypsPRO was used (2012) **Structure Solution and Refinement:** Crystal structure solution was achieved using direct methods as implemented in SHELXTL (v6.14)⁷³ or using the package SIR 2011⁷⁴ and visualized using the program XP. Missing atoms were subsequently located from difference Fourier synthesis and added to the atom list. Least-squares refinement on F² using all measured intensities was carried out using the program SHELXTL (v6.14).⁷³ All non hydrogen atoms were refined including anisotropic displacement parameters.

Acknowledgements:

The authors are grateful to the Spanish Ministerio de Educación y Ciencia (CTQ2010-14938/BQU, Consolider Ingenio 2010 and the Generalitat de Catalunya (for financial support 2009SGR116) and the Universitat Rovira I Virgili for awarding a research grant to Oriol Martínez (URV 2010PFR-URV-B2-01).

Notes and references

- ^a Institute of Chemical Research of Catalonia (ICIQ), Avgda. Paisos Catalans 16, Tarragona, Spain. E-mail: pvanleeuwen@iciq.es
^b Departament de Quí mica Física i Inorgànica, Universitat Rovira i Virgili, C/Marcel·li Domingo s/n, 43007 Tarragona, Spain; E-mail: carmen.claver@urv.cat
^c Department of Chemistry, Imperial College London, Exhibition Road, South Kensington, London, UK; E-mail: g.britovsek@imperial.ac.uk
^d Centre Tecnològic de la Quí mica, C/Marcel·li Domingo s/n, 43007 Tarragona, Spain
 carmen.claver@urv.cat

† Electronic Supplementary Information (ESI) available: [details of any supplementary information available should be included here]. See DOI: 10.1039/b000000x/

- L. R. Scolnick, Z. F. Kanyo, R. C. Cavalli, D. E. Ash, and D. W. Christianson, *Biochemistry*, 1997, **36**, 10558–65.
- E. A. Lewis and W. B. Tolman, *Chem. Rev.*, 2004, **104**, 1047–76.
- R. G. Wilkins, *Chem. Soc. Rev.*, 1992, **21**, 171–8.
- D. C. Johnson, D. R. Dean, A. D. Smith, and M. K. Johnson, *Annu. Rev. Biochem.*, 2005, **74**, 247–81.
- K. E. Liu, A. M. Valentine, D. Qiu, D. E. Edmondson, E. H. Appelman, T. G. Spire, and S. J. Lippard, *J. Am. Chem. Soc.*, 1995, **117**, 4997–8.
- H. Basch, K. Mogi, M. G. Djamaladdin, and K. Morokuma, *J. Am. Chem. Soc.*, 1999, **121**, 7249–56.

7. M. J. Jędrzejak and P. Setlow, *Chem. Rev.*, 2001, **101**, 607–18.
8. S. Friedle, E. Reisner, and S. J. Lippard, *Chem. Soc. Rev.*, 2010, **39**, 2768–79.
9. J. A. Osborn and R. R. Schrock, *J. Am. Chem. Soc.*, 1971, **93**, 2397–407.
10. T. G. Schenck, J. M. Downes, C. R. C. Milne, P. B. Mackenzie, T. G. Boucher, J. Whelan, and B. Bosnich, *Inorg. Chem.*, 1985, **24**, 2334–7.
11. J. Chatt and L. Venanzi, *J. Chem. Soc.*, 1957, 4735–41.
12. M. Green, T. Kuc, and H. Taylor, *J. Chem. Soc.*, 1971, 2334–7.
13. L. Nindakova, N. Chipanina, M. Turchaninov, and B. Shainyan, *Russ. Chem. Bull.*, 2005, **54**, 2343–7.
14. M. S. Viciu, R. F. Germaneau, O. Navarro-Fernandez, E. D. Stevens, and S. P. Nolan, *Organometallics*, 2002, **21**, 5470–2.
15. K. Severin, *Chem. Eur. J.*, 2002, **8**, 1514–8.
16. E. Dias and R. Grubbs, *Organometallics*, 1998, **17**, 2758–67.
17. Z. Freixa, P. C. J. Kamer, M. Lutz, A. L. Spek, and P. W. N. M. van Leeuwen, *Angew. Chem. Int. Ed.*, 2005, **44**, 4385–8.
18. D. R. Moore, M. Cheng, E. B. Lobkovsky, and G. W. Coates, *J. Am. Chem. Soc.*, 2003, **125**, 11911–24.
19. I. Guzei, K. Li, G. Bikzhanova, J. Darkwa, and S. Mapolie, *Dalton Trans.*, 2003, 715–722.
20. J. M. López Valbuena, E. Escudero-Adán, J. Benet-Buchholz, Z. Freixa, and P. W. N. M. van Leeuwen, *Dalton Trans.*, 2010, **39**, 8560–74.
21. D. Maiti, J. S. Woertink, A. A. N. Sarjeant, E. I. Solomon, and K. D. Karlin, *Inorg. Chem.*, 2008, **47**, 3787–3800.
22. Z. Weng, S. Teo, Z. Liu, and T. S. A. Hor, *Organometallics*, 2007, **26**, 2950–2.
23. O. Iranzo, T. Elmer, J. P. Richard, and J. R. Morrow, *Inorg. Chem.*, 2003, **42**, 7737–46.
24. D. McCollum and B. Bosnich, *Inorg. Chim. Acta*, 1998, **270**, 13–9.
25. B. Bosnich, *Inorg. Chem.*, 1999, **38**, 2554–62.
26. J. I. van der Vlugt, T. B. Rauchfuss, C. M. Whaley, and S. R. Wilson, *J. Am. Chem. Soc.*, 2005, **127**, 16012–3.
27. D. Fenton, *Chem. Soc. Rev.*, 1999, 159–68.
28. M. K. Richmond, S. L. Scott, G. P. a. Yap, and H. Alper, *Organometallics*, 2002, **21**, 3395–400.
29. S. J. Young, B. Kellenberger, J. H. Reibenspies, S. E. Himmel, M. Manning, O. P. Anderson, and J. K. Stille, *J. Am. Chem. Soc.*, 1988, **110**, 5744–53.
30. M. Haas, E. Solari, Q. T. Nguyen, S. Gautier, R. Scopelliti, and K. Severin, *Adv. Synth. Catal.*, 2006, **348**, 439–42.
31. L. A. Oro, M. A. Ciriano, and C. Tejel, *Pure Appl. Chem.*, 1998, **70**, 779–88.
32. E. Sola, V. I. Bakhmutov, F. Torres, A. Elduque, J. A. López, F. J. Lahoz, H. Werner, and L. A. Oro, *Organometallics*, 1998, **17**, 683–96.
33. M. A. Esteruelas, M. P. Garcia, A. M. Lopez, and L. A. Oro, *Organometallics*, 1991, **10**, 127–33.
34. A. L. Gavrilova and B. Bosnich, *Chem. Rev.*, 2004, **104**, 349–83.
35. S. Turba, O. Walter, S. Schindler, L. P. Nielsen, A. Hazell, C. J. McKenzie, F. Lloret, J. Cano, and M. Julve, *Inorg. Chem.*, 2008, **47**, 9612–23.
36. R. M. Haak, A. Decortes, E. Escudero-Adán, M. Martínez Belmonte, E. Martin, J. Benet-Buchholz, and A. W. Kleij, *Inorg. Chem.*, 2011, **50**, 7934–6.
37. M. Costas, X. Ribas, A. Poater, J. M. López Valbuena, R. Xifra, A. Company, M. Duran, M. Solà, A. Llobet, M. Corbella, M. A. Usón, J. Mahía, X. Solans, X. Shan, and J. Benet-Buchholz, *Inorg. Chem.*, 2006, **45**, 3569–81.
38. A. Company, J.-E. Jee, X. Ribas, J. M. López Valbuena, L. Gómez, M. Corbella, A. Llobet, J. Mahía, J. Benet-Buchholz, M. Costas, and R. van Eldik, *Inorg. Chem.*, 2007, **46**, 9098–110.
39. N. Pilkington and R. Robson, *Aust. J. Chem.*, 1970, **23**, 2225–36.
40. H. Adams, N. A. Bailey, P. Bertrand, C. O. R. de Barbarin, D. E. Fenton, and S. Gou, *J. Chem. Soc. Dalton Trans.*, 1995, 275–9.
41. J. Park and S. Hong, *Chem. Soc. Rev.*, 2012, **41**, 6931–43.
42. B.-S. Liao, Y.-H. Liu, S.-M. Peng, and S.-T. Liu, *Dalton Trans.*, 2012, **41**, 1158–64.
43. J. Gao, J. H. Reibenspies, and A. E. Martell, *Angew. Chem. Int. Ed.*, 2003, **42**, 6008–12.
44. R. Berg, J. Straub, E. Schreiner, S. Mader, F. Rominger, and B. F. Straub, *Adv. Synth. Catal.*, 2012, **354**, 3445–50.
45. B. M. Trost and T. Mino, *J. Am. Chem. Soc.*, 2003, **125**, 2410–1.
46. B. Trost and H. Ito, *J. Am. Chem. Soc.*, 2001, **123**, 12003–4.
47. Y. Yang, Y. Hayashi, Y. Fujii, T. Nagano, Y. Kita, T. Ohshima, J. Okuda, and K. Mashima, *Catal. Sci. Technol.*, 2012, **2**, 509–13.
48. W. Clegg, R. W. Harrington, M. North, and R. Pasquale, *Chem. Eur. J.*, 2010, **16**, 6828–43.
49. C. J. Whiteoak, E. Martin, M. M. Belmonte, J. Benet-Buchholz, and A. W. Kleij, *Adv. Synth. Catal.*, 2012, **354**, 469–76.
50. J. E. Dengler, M. W. Lehenmeier, S. Klaus, C. E. Anderson, E. Herdtweck, and B. Rieger, *Eur. J. Inorg. Chem.*, 2011, **2011**, 336–43.
51. M. A. Fuchs, T. A. Zevaco, E. Ember, O. Walter, I. Held, E. Dinjus, and M. Döring, *Dalton Trans.*, 2013, **42**, 5298–305.
52. J. Gao, Q.-W. Song, L.-N. He, C. Liu, Z.-Z. Yang, X. Han, X.-D. Li, and Q.-C. Song, *Tetrahedron*, 2012, **68**, 3835–42.
53. M. Taherimehr, S. M. Al-Amsyar, C. J. Whiteoak, A. W. Kleij, and P. P. Pescarmona, *Green Chem.*, 2013, **15**, 3083–90.
54. A. Buchard, M. R. Kember, K. G. Sandeman, and C. K. Williams, *Chem. Commun.*, 2011, **47**, 212–4.
55. M. Sunjuk, A. S. Abu-Surrah, E. Al-Ramahi, A. K. Qaroush, and A. Saleh, *Transit. Met. Chem.*, 2013, **38**, 253–7.
56. C. J. Whiteoak, E. Martin, E. Escudero-Adán, and A. W. Kleij, *Adv. Synth. Catal.*, 2013, **355**, 2233–9.
57. A. Banihashemi and A. Rahmatpour, *Tetrahedron*, 1999, **55**, 7271–8.
58. A. Banihashemi and A. Abdolmaleki, *Eur. Polym. J.*, 2004, **40**, 1629–35.
59. X. Sala, E. J. García Suárez, Z. Freixa, J. Benet-Buchholz, and P. W. N. M. van Leeuwen, *Eur. J. Org. Chem.*, 2008, **2008**, 6197–205.
60. J. T. Markiewicz, O. Wiest, and P. Helquist, *J. Org. Chem.*, 2010, **75**, 4887–90.
61. S. C. Bart, E. B. Lobkovsky, E. Bill, K. Wieghardt, and P. J. Chirik, *Inorg. Chem.*, 2007, **46**, 7055–63.
62. P. Shejwalkar, N. P. Rath, and E. B. Bauer, *Dalton Trans.*, 2011, **40**, 7617–31.
63. G. B. McGaughey, M. Gagne, and A. K. Rappe, *J. Biol. Chem.*, 1998, **273**, 15458–63.
64. M. O. Sinnokrot, E. F. Valeev, and C. D. Sherrill, *J. Am. Chem. Soc.*, 2002, **124**, 10887–93.
65. E. C. Constable, G. Baum, E. Bill, R. Dyson, V. Eldik, D. Fenske, S. Kaderli, D. Morris, A. Neubrand, M. Neuburger, D. R. Smith, K. Wieghardt, M. Zehnder, A. D. Zuberbühler, and R. van Eldik, *Chem. – A Eur. J.*, 1999, **5**, 498–508.
66. Y. Zang, J. Kim, Y. Dong, E. C. Wilkinson, E. H. Appelman, and L. Que, *J. Am. Chem. Soc.*, 1997, **119**, 4197–205.
67. V. Calo, A. Nacci, A. Monopoli, and A. Fanizzi, *Org. Lett.*, 2002, **4**, 1552–4.
68. Y. Zhao, J.-S. Tian, X.-H. Qi, Z.-N. Han, Y.-Y. Zhuang, and L.-N. He, *J. Mol. Catal. A: Chem.*, 2007, **271**, 284–9.
69. S. R. Choon, J. Hwang, B. L. Hong, and J. J. Shim, *B. Kor. Chem. Soc.*, 2007, **28**, 1060–2.
70. J.-Q. Wang, K. Dong, W.-G. Cheng, J. Sun, and S.-J. Zhang, *Catal. Sci. Technol.*, 2012, **2**, 1480–4.
71. F. Castro-Gómez, G. Salassa, A. W. Kleij, and C. Bo, *Chem. Eur. J.*, 2013, **19**, 6289–98.
72. O. Martínez-Ferraté, G. J. P. Britovsek, C. Claver, and P. W. N. M. Van Leeuwen, *Inorg. Chim. Acta*, 2015, ASAP.
73. G. M. Sheldrick, *Acta Cryst.*, 2008, **64**, 112–22.
74. M. C. Burla, R. Caliendo, M. Camalli, B. Carrozzini, G. L. Casciaro, C. Giacovazzo, M. Mallamo, A. Mazzone, G. Polidori, and R. Spagna, *J. Appl. Crystallogr.*, 2012, **45**, 357–61.